Structure-Property Behavior of Elastomeric Segmented PTMO–Ionene Polymers. II

D. FENG, L. N. VENKATESHWARAN and G. L. WILKES,
Polymer Materials and Interfaces Laboratory and Department of Chemical Engineering, Virginia Polytechnic Institute and State University, Blacksburg, Virginia 24061-6496, and
CHARLES M. LEIR and JOHN E. STARK,
Speciality Chemicals Division, 3M Company, St. Paul, Minnesota 55144

Synopsis

A series of segmented ionene polymers based on the reaction of α,ω-bis(dimethyl amino)polytetramethylene oxide with various dihalide compounds were investigated with respect to their structure–property behavior. The placement of quaternary ammonium ions and halide counterions along the polymer chains was varied by changing the molecular weight of the PTMO soft segment and the structure of the dihalide linking agent. The techniques of dynamic mechanical spectroscopy, thermal analysis, small angle X-ray scattering, and stress–strain behavior analysis were applied. For the case when the PTMO soft segment was amorphous, the ambient temperature properties of these materials displayed low modulus, high strength, and high elongation elastomeric behavior with tensile strength enhanced by the strain-induced crystallization of the PTMO. A high level of phase separation existed between the dihalide component relative to the PTMO soft segment. Due to the Coulombic association of the ionene species, these materials displayed many similarities to the segmented urethane ionomers. In particular, distinct domain structure was noted by SAXS, whose dimensional scale was similar to the segmented urethanes. It was also shown, however, that the driving forces for the microphase separation was caused by favorable electrostatic or Coulombic interactions in contrast to segment–segment incompatibility features as in the segmented urethanes.

INTRODUCTION

As described in the previous paper, a series of segmented ionene elastomeric materials have been prepared which suggest strong association or domain formation of the ionene groups.[1] These segmented polymers represented by the generalized structure of Scheme I are based on the reaction of α,ω-bis(dimethylamino) poly(tetramethylene oxide) (PTMO) with various dihalide compounds. In the case of Scheme I, a dibenzyl halide structure is shown having a spacer group denoted as Y, but other related systems have also been prepared[1].

These materials display a rather high softening temperature of the order ca. 150–180°C (TMA) and utilize a soft segment based on poly(tetramethylene oxide) (PTMO) which can be controlled in its segment molecular weight. PTMO is well known as a soft segment in thermoplastic elastomers such as the segmented urethanes, segmented urethane-ureas, etc. to display strain-induced crystallization. This event can help enhance tensile strength as will be demonstrated in the work discussed in this paper. However, if the PTMO soft segment is of sufficient molecular weight, it may lead to crystallization at

Journal of Applied Polymer Science, Vol. 37, 1549–1565 (1989)
 CCC 0021-8995/89/081549-17$04.00

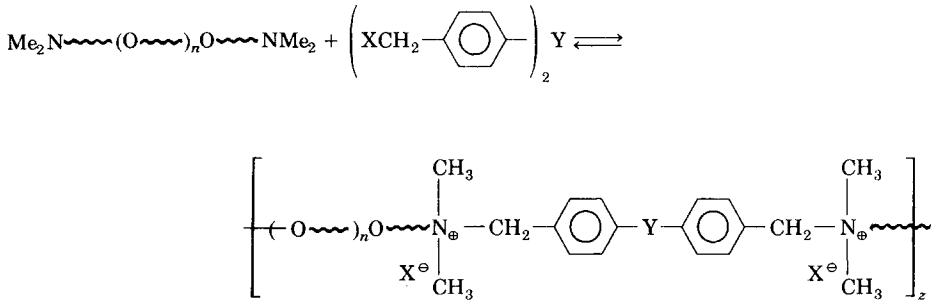

Scheme I

ambient temperature which may be viewed as a disadvantage if indeed the material is to be considered as a thermoplastic elastomer. Specifically, soft segment crystallization will lead to a loss of elastomeric character as ambient aging occurs—a topic that will be addressed in discussing further details of the properties of the systems reported in the preceeding paper.

As a point of interest, the use of ionene moieties provides a somewhat unique route for the preparation of new segmental thermoplastic elastomers which differs from the general domain, forming segmented urethane or segmented urethane–urea systems. In these latter conventional materials the average hard segment must generally contain more than one hard segment moiety for establishing sufficient microphase separation necessary for enhancing physical properties. In the case of the ionenes, however, and as will be illustrated, one can obtain good phase separation with a single unit of the ionene containing moieties utilized in the synthesis of the polymers discussed in this paper. There is, of course, much similarity of the ionene structures discussed here to those of the elastomeric ionomers.[2,3] Clearly ionenes can be viewed somewhat as a subclass of these systems provided that the ionene content is of relatively low mole percent. In fact, the ionenes would be expected to have many of the same behavioral features as the so-called segmented urethane anionomers introduced by Dietrich and co-workers[4] and more recently addressed in their structure–property behavior as based on the work of Hwang et al.,[5] Rutkowska and Eisenberg,[6,7] and Rutkowska.[8] Specifically, these materials tend to display a pseudo-elastomeric network behavior where both the ionic interactions and the "hard segments" establish a highly cohesive microdomain morphology.[5] With this information in mind, further details of the structure–property relationships of selected materials prepared by the routes described in the previous paper will now be addressed. The specific objectives of this work will be to present information accounting for the characteristics of these ionenes as a function of:

(a) the molecular weight of the PTMO soft segment
(b) the counter ion of the ionene moiety (Br^- vs. Cl^-)
(c) architectural differences of the ionene hard segment component
(d) influence of charge on promoting phase separation

TABLE I
List of Ionene Samples

Sample	IV[a] (0.4 g/dL)	Ionic conc (%) (per PTMO repeat unit)	Dihalide (mol %) (per PTMO repeat unit)	TMA softening temperature[a] (°C)
IB-NS-34	1.31	4.26	2.13	179
IB-NS-35	1.10	4.11	2.06	179
IB-NS-38	1.37	3.77	1.89	179
IB-NS-65	1.90	2.22	1.11	179
IB-NS-66	2.13	2.17	1.09	179
IB-NS-100	2.23	1.44	0.72	179
IB-S-34	1.57	4.26	2.13	157
IB-S-65	3.50	2.22	1.11	157
IB-S-66	2.77	2.17	1.09	157
IB-S-100	2.62	1.44	0.72	157
IC-NS-34	2.40	4.26	2.13	157
IC-NS-35	1.40	4.11	2.06	157
IC-NS-38	1.32	3.77	1.89	157
IC-NS-66	2.52	2.17	1.09	157
IC-NS-100	3.20	1.44	0.72	157
IC-S-65	1.90	2.22	1.11	N/A
IC-S-66	2.35	2.17	1.09	N/A
IC-S-100	2.48	1.44	0.72	N/A

[a] From Ref. 1.

EXPERIMENTAL

The experimental details regarding the synthesis of the ionenes in this paper have been presented in the preceeding paper (Part I).[1] The specific materials that were selected here for investigation have been listed in Table I along with some of their characteristics—some of which were obtained by their initial characterization discussed in Part I. As provided in this table, it is observed that the level of ionic content is of the order of magnitude of what is found in the elastomeric ionomers,[2,3] i.e., a few mole percent. It is particularly important to note the scheme by which samples will be designated as can be obtained from Scheme II.

In addition to the ionene systems, the synthesized unchanged "analog" chain structure discussed in Part I was also investigated by small angle X-ray scattering in this study; see Scheme III.

Mechanical Properties. General stress–strain characterization including cyclic hysteresis and stress–relaxation were conducted either on an Instron (Model 1122) or a Tensilon (Model UTM-II), all at ambient conditions. Limited creep measurements were also determined at ambient temperature using an initial stress to promote an elongation of about 6%. Changes in strain were monitored with a cathetometer. Higher temperature mechanical behavior will be reported in a separate paper. Dog-bone-shaped samples measuring 10 mm in length and 2.8 mm in width were cut from chloroform solution cast films. These films had been well dried and stored under vacuum (until tested) to remove any traces of solvent. For the hysteresis measurements, increments of 50% elongation were utilized on the dog bone samples stated above. The respective crosshead speeds during loading and unloading were 50 mm/min.

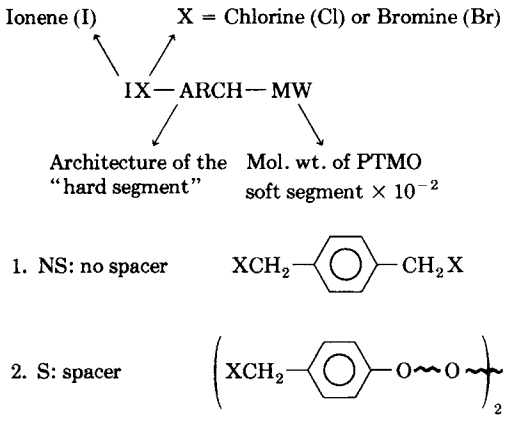

Scheme II.

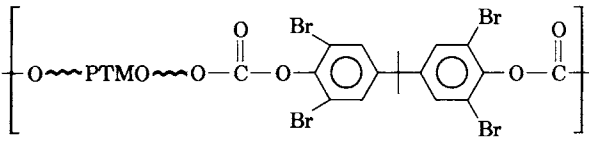

Scheme III.

Dynamic Mechanical Spectroscopy. An autovibron viscoelastometer was used to measure the real part of the dynamic modulus E', the loss modulus E'', and tan δ at a heating rate of 2°C/min. These parameters were determined as a function of temperature (−150–200°C) at a frequency of 11 Hz.

Thermal Analysis. Both differential scanning calorimetry (DSC) and thermal mechanical analysis (TMA) were carried out on these materials. The DSC results were obtained utilizing a Perkin-Elmer DSC-4 with the materials investigated over the range of 20–180°C at a scan rate of 10°C/min. The TMA analysis was discussed in Part I and a portion of that data obtained at a scan rate of 10°C/min will be readdressed within this paper.

X-Ray Analysis.

(A) *Wide angle X-ray scattering* (*WAXS*): All WAXS results were obtained utilizing a Philips tabletop X-ray generator Model PW1170 equipped with a standard vacuum sealed Warhus photographic pinhole camera. The exposure times for cast films varied from 16 to 20 hours, depending on the film thickness. To study the occurrence of strain-induced crystallinity, 10 mm samples were strained at ca. 50 mm/min to 700% elongation, clamped to a rigid sample holder and mounted in the Warhus camera for analysis.

(B) *Small angle X-ray scattering* (*SAXS*): A standard Kratky slit collimated camera was used for the SAXS experiments. The X-ray source was from a Siemens AG Cu 40/2 tube operated at 40 kV and 20 mA by a GE XRD-6 generator. Copper K_α radiation of wavelength 1.542 Å was obtained by nickel foil filtering. The scattered intensity was monitored by a 1-dimensional position sensitive detector (M. Braun–Innovative Technology Inc.).

RESULTS AND DISCUSSION

Due to the fact that the higher molecular weight PTMO containing materials could show soft segment crystallization upon aging (see later discussion), the materials were initially heated to 60°C for 1–2 h for purposes of completely melting out any possible PTMO crystallinity. The general stress–strain measurements were then made once the samples had been returned to ambient for a short period.

General Stress–Strain Behavior. Figure 1 illustrates the general stress–strain curves that were obtained for the materials all synthesized with the dibenzyl bromide—recall Table I and Scheme II. Each curve represents the general behavior for several samples tested of a given designation. It is noted that these systems display significant elongation at break (ca. 1000%) under the testing conditions utilized. It was sometimes found that slippage at the clamps did occur and indeed obtaining the ultimate elongation was somewhat difficult but with careful measurement, the values indicated in Figure 1 are clearly indicative of their ultimate behavior. It is also noted that the tensile strength is of the order of 40 MPa in all cases, which is quite significant for elastomeric materials.

It is observed that there is a distinct upturn in the stress when elongations of the order of 500–600% elongation are exceeded. While this increased stress level could be indicative of general non-Gaussian behavior due to extension of the PTMO soft segments, it is primarily due to the contribution of strain-induced crystallinity of the PTMO soft segments, as will be pointed out in a later section addressing crystallization via wide angle X-ray scattering.

The Young's moduli of these materials are given in Table II along with other ionenes that were investigated in this study, but for which all the stress–strain curves are not presented due to their rather strong similarity to those given in Figure 1. This table provides both the modulus of a given sample as determined after the heat treatment to remove any PTMO crys-

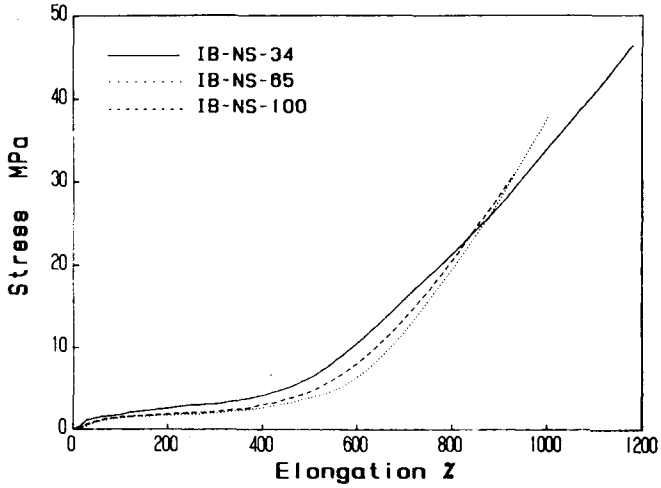

Fig. 1. Effect of PTMO soft segment molecular weight on the stress–strain behavior of the IB-NS series: (—) −34; (···) −85; (- - -) −100.

tallinity ("fresh") as well as the modulus of the same material after aging at ambient over 3 weeks ("aged") where the influence of PTMO crystallinity is observed. For comparison of the different counterions, i.e., bromine vs. chlorine, and to also note the effect of the spacer group in the dihalide moiety, Figure 2 presents three typical stress–strain curves obtained for the samples so designated. These results, which are again typical for these materials, illustrate that when the counterion is chlorine, other factors being as constant as possible, there is a general increase in the stress at a given elongation relative to those containing bromine—at least at elongations exceeding 50%. There is no major difference in tensile strength, but it did appear that, at an equivalent elongation, the systems possessing chlorine as the counterion consistently provided somewhat higher stress values relative to those containing bromine counterions. As a speculation, this difference may be due to the smaller and more electronegative chlorine (3.2 eV) in contrast to bromine (3.0 eV)[9] and which may therefore promote better packing and coulombic interactions with the ionene species, thereby providing stronger association.

In noting the effect of the spacer group (recall Scheme I) on property behavior, Figure 2 also provides information on this topic. These results indicate that when the aliphatic ether containing spacer group is within the dihalide hard segment, other structural factors being constant, the material shows a lower stress at a given elongation than in the absence of the spacer. This was typical for other ionene systems when analogous structures were compared with and without spacer. It is speculated that this arises due to the fact that there is a weaker association of the ionene moieties caused by the more aliphatic character and thereby somewhat poorer phase separation in the IB-S and IC-S materials. However, these differences may be simply due to

TABLE II
Young's Modulus of Ionene Samples Determined at 23°C

Sample	Young's modulus (MPa)	
	Fresh[a]	Aged[b]
IB-NS-34	4.1	4.3
IB-NS-35	2.7	35.2
IB-NS-38	3.5	3.3
IB-NS-100	3.1	62.7
IB-S-34	3.5	8.6
IB-S-65	2.6	27.0
IB-S-66	2.3	56.8
IB-S-100	3.1	50.1
IC-NS-38	3.9	3.3
IC-NS-66	3.3	12.2
IC-NS-100	3.6	49.2
IC-S-65	2.7	50.4
IC-S-66	1.8	32.0
IC-S-100	2.6	48.6

[a] Values obtained after holding the sample at 60°C for 1–2 h and quenching to ambient.
[b] Values obtained after the sample had been aged at ambient temperature for at least 1 month.

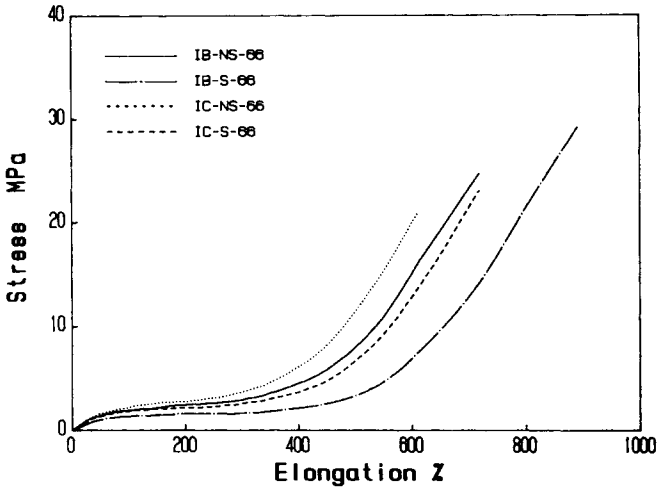

Fig. 2. Effect of counterion as well as the chemical structure of the "hard segment" on the stress–strain behavior of selected halo-ionenes having a PTMO segment molecular weight of 3400: (—) IB-NS-66; (– · –) IB-S-66; (· · ·) IC-NS-66; (- - -) IC-S-66.

poorer association rather than due to a higher degree of hard–soft segment mixing as might be expected due to the greater similarity in hard and soft segment solubility parameters when the spacer is present. There is also a third possible explanation that may be relevant. Specifically, for those systems containing a spacer, we have constructed a molecular space filling model of the overall hard segment and have found that the benzyl halide of one end of the hard segment can fold over and interact with the other benzyl halide due to the flexible ether linkage. This suggests that there may be some "kinks" placed into the chain which indeed would help account for the lower stress behavior at a given elongation of those ionene materials containing a hard segment with the spacer. As will be indicated in a later paper utilizing small angle X-ray scattering, although there is a slight increase in the degree of interfacial character (interphase mixing) when the spacer group is present, the increase is still quite small relative to the materials with no spacer and thus we must speculate that any differences between those polymers containing a spacer more likely arise from a lesser ability to form strong and possibly multiple ionic associations. An additional comparison that can be viewed in Figure 2 is that the chlorine-containing counterions tend to provide a somewhat lower degree of elongation than those containing bromine. Recall, however, that for a given level of elongation attained, the chloride systems provide a higher stress level—other structural features being constant.

The mechanical hysteresis data obtained on samples IB-NS-34, IB-NS-35, IB-S-34, and IC-NS-35 are given in Figure 3 and illustrate that, at the temperature used for this measurement and at these loading and unloading rates, there is relatively little difference in their dissipative character. It might be pointed out, however, that the percent hysteresis is relatively high for extensions exceeding 300%—at least as compared to elastomeric sulfonated telechelic polyisobutylene ionomers investigated in this same laboratory under the same test conditions.[10] However, in these latter systems, the stress levels

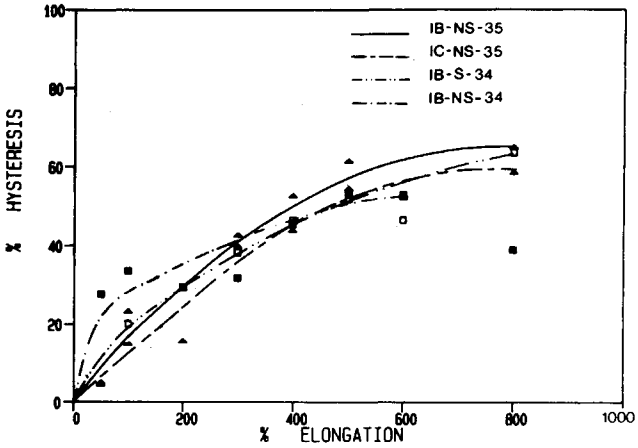

Fig. 3. Mechanical hysteresis vs. percent elongation for the halo-ionenes studied: (—) IB-NS-35; (— - —) IC-NS-35; (— · · —) IB-S-34; (— · —) IB-NS-34.

achieved were considerably less than those of the ionenes even though the general mole percent of ionic moieties were of the same magnitude. The hysteresis behavior observed here for ionene systems does more closely parallel that found for many conventional thermoplastic segmented polyurethanes —also investigated in this laboratory.[11]

Figure 4 provides a typical example of the general ambient temperature stress–relaxation behavior (at 25% elongation) and creep response—the latter of which utilized an initial stress level that promoted a 6% elongation. The time period over which these two tests were run on sample IB-NS-100 was about 16 days. Both types of data clearly illustrate that this ionene material displays a strong pseudonetwork behavior for the linear rubbery material since there is only an order of a 50% decrease in stress and doubling of the

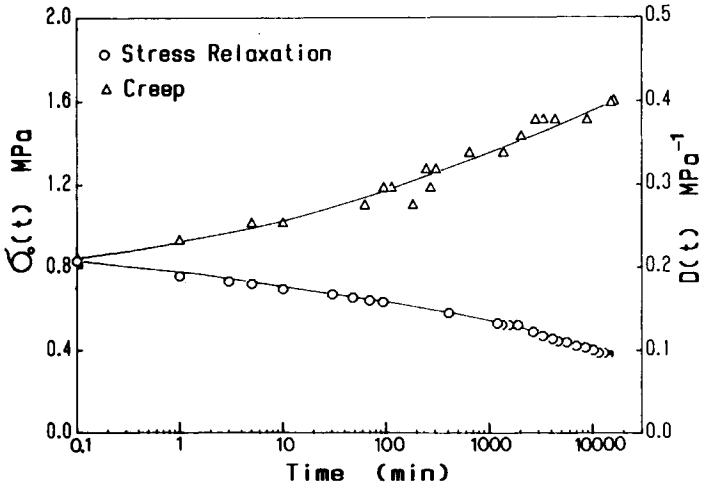

Fig. 4. Stress relaxation (at 25% elongation) (∘) and tensile creep (△) response of IB-NS-100 ionene determined at 23°C.

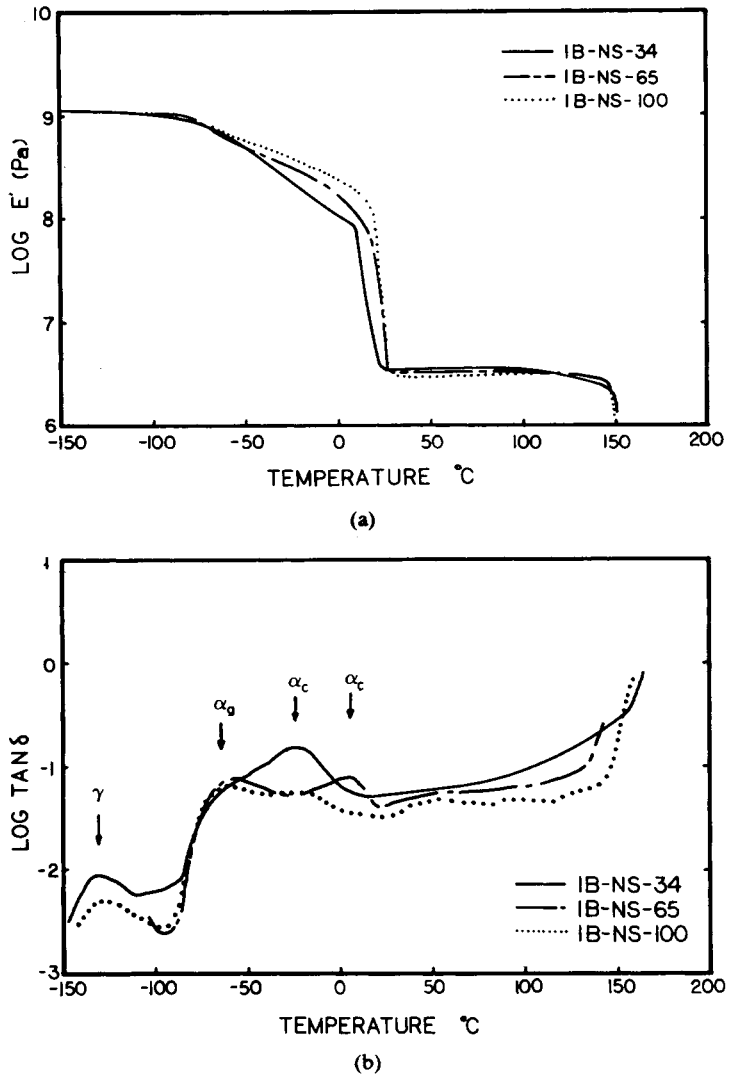

Fig. 5. Effect of PTMO soft segment molecular weight on the dynamic mechanical response of the IB-NS series: (—) −34; (— — —) −65; (· · ·) −100; (a) storage moudulus (E'); (b) tan δ, (E''/E').

creep compliance over this many day period. Indeed, in again contrasting these results with similar measurements carried out on the sulfonated telechelic polyisobutylene ionomers mentioned earlier, the ionene systems display much better long-term network response. Also, when compared against similar behavior for many of the thermoplastic segmented or block polymers, the response of the ionene is particularly good in terms of its limited viscoelastic flow.

Dynamic Mechanical Behavior. Figures 5(A) and (B) provide some of the dynamic mechanical spectra obtained on selected ionenes of the IB-NS series. The principal variable is that of the PTMO soft segment molecular weight,

which varies from 3400 to 10,000. From these data, three principal transitions were observed for all samples. The transition occurring at −120°C was designated as the γ-relaxation, which was observed in all ionenes. This transition is strongly believed to arise from the methylene sequencing in the soft segment and is in excellent agreement with the reported values for this same transition observed in polymers possessing methylene sequences in the backbone.[12] Indirectly, the observation of this transition occurring where it is expected does at least *suggest* that the degree of phase separation of the soft segment from the ionene moieties may be very high, thereby supporting the earlier statements regarding phase separation.

A second transition occurs around −70°C and has been designated α_g, which is distinctly attributed to the glass transition temperature of PTMO. As the data illustrate, the location of the onset of α_g for all of the IB-NS ionenes shown is essentially the same (ca. −70°C). Since the values for pure PTMO is expected to be in this range, this transitional response also strongly suggests that there is little mixing of the PTMO with the ionene dihalide hard segments. This observation is in line with our earlier comments concerning mixing as based on the γ transition.

A third transition region denoted as α_c is related to the general crystallization and melting behavior of the PTMO soft segment. It was found that the intensity of α_c increased as the PTMO molecular weight decreased, which suggests that shorter PTMO chains appear to undergo less crystallization—at least during the *initial* sample cooling. The cause for the decreasing modulus extending from nearly −70 to 25°C is undoubtedly due to the initial softening of the amorphous PTMO in conjunction with the melting of PTMO crystallinity—the latter effect is quite pronounced for the E' behavior in the range of ca. 25°C [see Fig. 5(A)].

There is actually a fourth transition at ca. 150°C but which is not completed within the tan δ results due to the loss of sensitivity of the instrument in this temperature range. This is the region where the material displays significant softening due to the loss of association of the ionene moieties and in fact where there is likely a decrease in the molecular weight due to reversion to the initial reactants—the dimethyl amino terminated PTMO and the dihalide compound, as was discussed in the preceeding paper. It is noted that a major decrease in modulus occurs at about the same temperature for all of the IB-NS compounds and, in fact, the softening occurs at nearly the same temperature for all the ionenes investigated. This large decrease in modulus or softening behavior occurs at a somewhat lower temperature than that determined in Part I utilizing TMA analysis. This difference is likely due to the lower scan rate used for the autovibron measurements (2°C/min) relative to the higher rate in the TMA analysis (10°C/min) and due to the general nature of the two types of tests as well as the way softening is defined in each. In summary of this upper transition, according to the autovibron analysis, this rapid decrease in modulus occurs at a temperature nearly independent of both the type of counterion and architecture of the ionene moieties.

It is noted that the value of E' in the rubbery plateau region (ca. 25–100°C) increases with a decreasing PTMO molecular weight. This behavior is consistent with the modulus from the stress–strain results and is expected since the

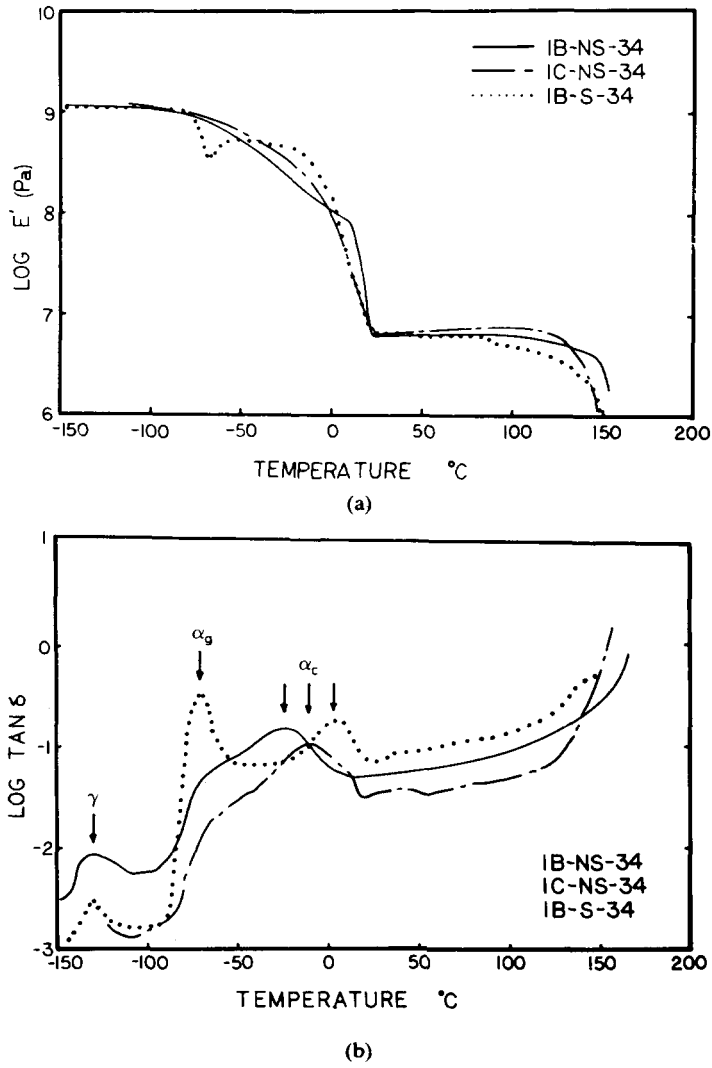

Fig. 6. Effect of the counterion as well as the chemical structure of the "hard segment" on the dynamic mechanical response of selected halo-ionenes: (—) IB-NS-34; (—·—) IC-NS-34; (· · ·) IS-S-34; (A) storage moudulus (E'); (B) tan δ, (E''/E').

lower molecular weight PTMO soft segment leads to a lower molecular weight between ionene groups or domains (physical or virtual crosslinks). At the same time, for the same dihalide moiety, a lower PTMO molecular weight also means a higher fraction of the volume will be occupied by the hard segment "reinforcing component."

In again comparing counterions as well as the effect of spacer for a given counterion, Figures 6(A) and (B) illustrate E' and tan δ for the respective samples of IB-NS-34, IC-NS-34, and IB-S-34. The behavior of E' illustrates the fact that the effect of a spacer promotes a more distinct glass transition observation for the PTMO soft segment. Specifically, as illustrated in Figure

6(A), the decrease in E' in the range of $-70°C$ and subsequent increase (due to crystallization) always occurred for the dihalide compound containing the spacer but not for those without. This implies that these latter systems crystallized less during the cooling process but had sufficient time to undergo crystallization during the heatup which caused the rise in E' to occur above T_g. However, the general melting characteristics of the PTMO were the same for all samples as expected.

Another distinctly obvious difference arose between those systems containing the spacer relative to those without, as can be observed by comparing the behavior in the rubbery plateau region of Figure 6(A). Specifically, while the ambient temperature modulus of the ionenes containing a spacer were nearly the same as those without spacer, as the temperature increased, those containing the spacer clearly showed the onset of modulus decrease or softening at a lower temperature. The "major degree of softening" for all systems was still ca. 150°C. Again, this behavior is in agreement with the initial stress–strain results discussed earlier, where it was speculated that the dihalide systems containing the spacer likely provide weaker overall association of the ionene domains, leading to a decrease in the general modulus characteristics as clearly supported by the dynamic mechanical data in Figures 6(A) and (B).

Thermal Analysis. The general softening characteristics as given by the TMA data presented in the preceeding paper indicate the loss of association of the ionene moieties and even the initiation of "depolymerization" of the initial reactants as higher temperatures are approached—see Part I and Table I of this paper. However, use of DSC has helped further confirm the occurrence of PTMO crystallization, particularly for those samples that undergo ambient aging. As an example of this response, Figure 7 illustrates three DSC scans of sample IB-NS-100 obtained at different times. The initial scan (A) was determined after the material had been aged at ambient conditions for approximately 2 months. As is clear, there is a distinct endothermic response which comes from the melting behavior of PTMO and which at this scan rate

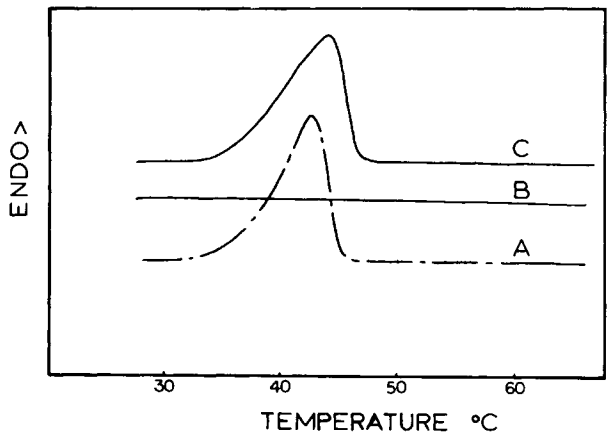

Fig. 7. DSC thermograms of IB-NS-100 ionene at the specified conditions: (A) scan of an aged sample; (B) quick rescan of sample A; (C) scan of sample B after a 30 days aging at 23°C.

(10°C/min) shows a T_m peak occurring at somewhat above 40°C, but the melting clearly begins below this temperature. These DSC data give clear support to the earlier dynamic mechanical observations where a significant softening occurs in the range of 25–35°C and which was explained by the melting of PTMO soft segments. [In the case just discussed, however, the crystallization of the PTMO was induced by aging at ambient conditions in contrast to the inducement caused by cooling the samples within the autovibron chamber which provides a higher driving force due to an increased supercooling]. The second DSC scan, labeled B in Figure 7, was obtained immediately after cooling the sample that had provided scan A. There is no sign of PTMO melting and, indeed, it takes a considerable period of time (several days) at ambient temperature for the crystallization to be reinduced. An example of this is shown in scan C of Figure 7, where the material that had provided scans A and B was aged at ambient for nearly 30 days and then this third DSC scan was obtained. It is noted that PTMO crystallization has indeed been reestablished, as would be expected. As also anticipated, for the lower molecular weight PTMO segments, it took longer for recrystallization to occur at ambient.

Further confirmation of PTMO crystallization was obtained by utilizing wide angle X-ray scattering and is illustrated in Figure 8(A). Clearly the WAXS pattern obtained on sample IB-NS-100 shows the development of PTMO crystallinity and occurs *if* a sufficient ambient temperature aging time is utilized. This time period is, of course, a function of the PTMO molecular weight, i.e., a higher PTMO soft segment molecular weight more readily undergoes ambient crystallization.

Utilizing the WAXS technique, the effect of strain for inducing PTMO crystallization, could also be readily demonstrated as is indicated in Figure 8(B). This figure shows the WAXS pattern obtained on a stretched sample of IB-NS-100 and the presence of oriented PTMO crystallites is readily apparent. The observed reflections match with those of oriented PTMO and hence this result clearly supports the earlier comments relating to the enhancement of the tensile strength caused by strain-induced crystallization of the soft segments.

Small Angle X-Ray Scattering and Microdomain Formation. To confirm the occurrence of the microphaselike separation heretofore proposed for these materials, SAXS profiles were obtained on all materials investigated. This scattering behavior, however, was obtained only after the materials had first been heated to 60°C for at least 2 h to remove all PTMO crystallinity, if any existed initially. As stated earlier, no signs of PTMO crystallization occurred for the order of days following this initial heating cycle. Hence, the SAXS studies allowed the investigation of domain formation since it was anticipated that, due to the large difference in electron density of the ionene-containing hard segments relative to the PTMO soft segments, if domain formation did develop, there was the possibility of observing a shoulder or peak in the SAXS profile. Indeed, as Figure 9(A) illustrates for sample IB-NS-38, there is a very distinct scattering peak observed in these systems with the smeared spacing (pseudo-Bragg spacing) being of the order of 100 Å and which systematically increases in a given series (data not shown) as the

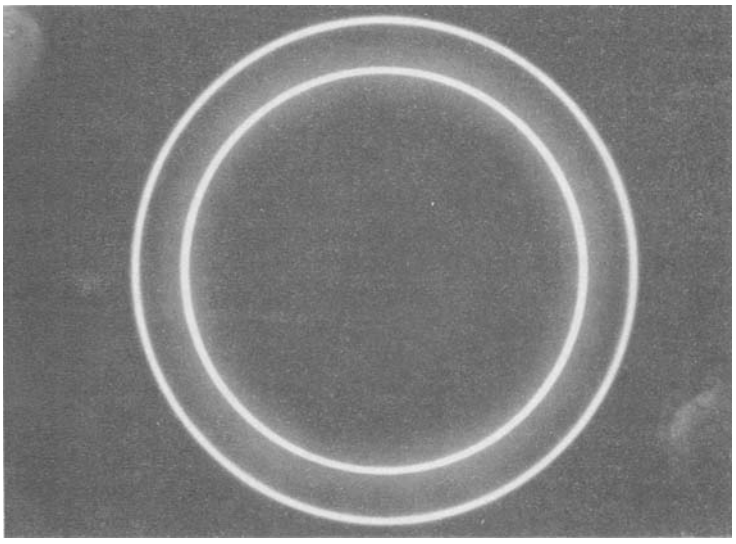

(a)

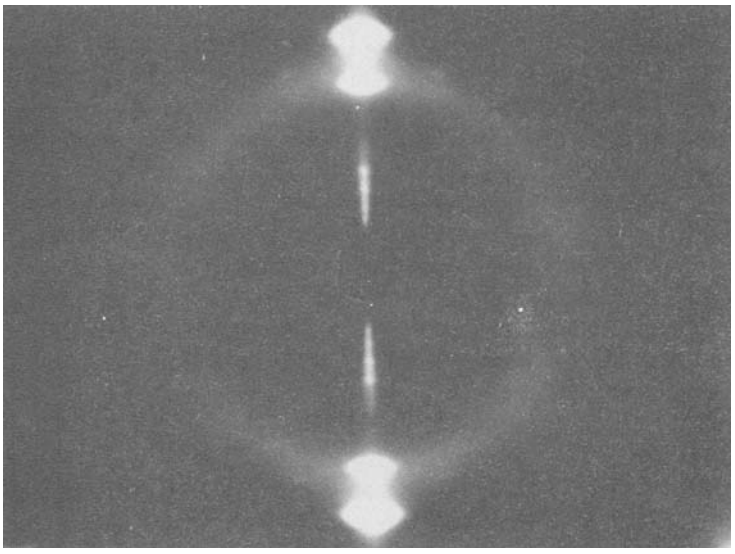

(b)

Fig. 8. WAXS pattern obtained for sample IB-NS-100: (A) after aging at ambient for 30 days; (B) after strain induced crystallization of an initially amorphous material that has been rapidly drawn to 700% elongation. The draw direction is along the horizontal axis.

molecular weight of the PTMO soft segment increases. This SAXS profile gives strong support for the presence of microphase separation of the ionene components, leading to the development of a distinct interference periodicity or correlation distance.

Further details of the analysis of the SAXS profiles will be provided in a later paper, but it seems appropriate to briefly mention some results obtained

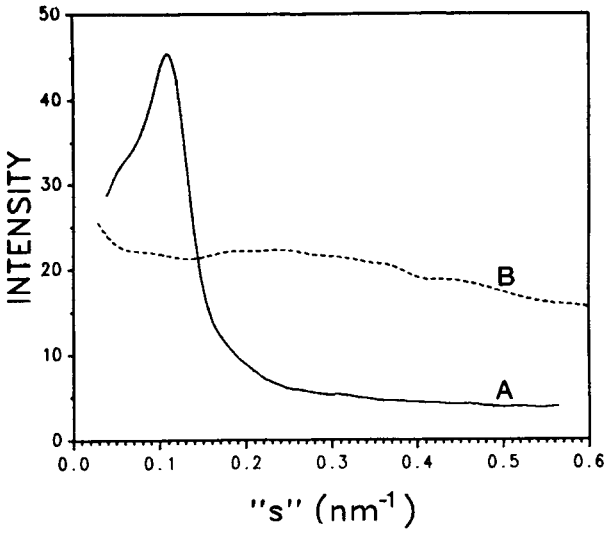

Fig. 9. Smeared SAXS scans as a function of the angular variable s. [$s = 2/\lambda$ (sin($\theta/2$))], where θ is the radical scattering angle: (A) ionene sample IB-NS-38; (B) segmented polymer containing the uncharged tetrabromo bisphenol hard segment.

by carrying out a Porod analysis of the higher angular scattered intensity (the tail of the SAXS profile). Specifically, negative deviations from Porod's law were observed, which were, however, of a relatively minor nature. Analysis of these data led to the determination of only a small degree of "hard segment–soft segment" interfacial thickness, ca. 1–2 Å for those ionenes without spacer whereas those containing a spacer provided a value of about 3–5 Å. Indeed, this would be expected on the basis of the observed properties, for *if* a high degree of interfacial thickness existed within these materials, this would imply that considerable mixing of the single hard segment units connecting with the PTMO soft segments would be present and this type of hard-soft segment mixing would not have been expected to provide the observed properties. In particular, as we have shown, all the ionene materials displayed: (a) high elongation–high strength behavior; (b) a low PTMO T_g; (c) a distinct low temperature γ-relaxation at ca. -120°C, expected of the methylene sequences; and finally (d) a distinct SAXS peak. All these features together strongly suggest that the degree of mixing of PTMO with the dihalide moieties is quite minimal. Again, further details of the SAXS analysis of these and other of the ionenes synthesized will be discussed in a subsequent publication.

As was discussed in Part I of this two-part series, a related segmented PTMO polymer was prepared which, however, contained no charge in the backbone (recall Scheme III). This system was first synthesized by reacting hydroxyl-terminated PTMO of 2000 molecular weight with phosgene to make the corresponding PTMO bischloroformate. This product was then reacted with tetrabromobisphenol under appropriate stoichiometry to achieve a high molecular weight polymer, as was characterized by its inherent viscosity of 1.43 (0.4 dL/g in chloroform at 30°C). As pointed out in Part I of this series,

this noncharged material indicated little or no phase *separation* as suggested by its lack of elastomeric behavior and at the same time by its TMA response, which illustrated that its softening point was of the order of 20°C as it was heated from liquid nitrogen temperatures. The reason for its rigidity at low temperatures simply extends from the semicrystalline character of the PTMO segment which melts near ambient. In this paper, we also address this same material for purposes of illustrating that phase separation is not present by a more direct method. In particular, the use of SAXS has been applied to this system and, while its hard segment content is higher than those ionene systems, we have also maintained a large electron density contrast by the presence of four bromine atoms per hard segment in comparison to two bromines per ionene segment in the earlier discussed systems. The SAXS scan of this material is shown in Figure 9(B)—this scan also being obtained by passing the beam normal to the film plane. It is noted that there is no indication whatsoever of the inducement of microphase separation in this uncharged but relatively similar chemical structure to that of the earlier ionene containing materials—compare with Figure 9(A). Certainly the low and monotonically decreasing scattering behavior also suggests a rather homogeneous system on this scale probed by the SAXS technique. Hence, these data lend strong proof to the suggestion provided in Part I that it is the charged quaternary ammonium groups within the backbone (and the corresponding anion) that promotes the phase separation driven on the basis of Coulombic interaction.

CONCLUSIONS

In summary of the work presented, these segmented ionene materials display many of the characteristics common to the segmented and block polymer thermoplastic elastomers. There are also strong similarities to the elastomeric ionomers that have been discussed in the literature. In fact, there are particularly strong similarities in behavior to the so-called urethane anionomers discussed by Dietrich and co-workers[4] and more recently by Hwang et al.,[5] Rutkowska and Eisenberg,[6,7] and Rutkowska.[8] We have shown, however, that in our case, the "domain character" is promoted by Coulombic interactions in contrast to simple segment–segment incompatibility as the basic driving force for more block and segmented polymers. The disappointing feature with regard to the systems discussed here is that they tend to degrade or possibly depolymerize when exposed to higher temperatures. While partial recovery is obtained through a "repolymerization mechanism," complete recovery of molecular weight does not appear to occur. Possibly through modification of the type of ionene chemistry discussed here, such reversibility in depolymerization–repolymerization might be promoted which indeed would enhance the potential commercial utility of such materials as thermoplastic elastomers. Presently, however, these systems can be applied to provide elastomeric high tensile strength behavior through means of solution coating. A further limitation of the materials discussed here is that when the PTMO segment is sufficiently long, crystallization of the "soft segment" can occur. This indeed leads to a rise in modulus with time and therefore alters the mechanical behavior. Again, through different choices of

soft segment chemistry, this behavior could likely be minimized or completely eliminated.

One of the author's (G.L.W.) would like to acknowledge the partial financial support of this work by the American Chemical Society Petroleum Research Fund (Grant #15441-AC7).

References

1. C. M. Leir and J. E. Stark, to appear.
2. Y. Mohajer, S. Bagrodia, G. L. Wilkes, R. F. Storey, and J. P. Kennedy, *J. Appl. Polym. Sci.*, **29**, 1943 (1984).
3. H. Makowski, R. D. Lundberg, L. Westerman, and J. Bock, in *Ions in Polymers*, A. Eisenberg, Ed., Adv. in Chem. Series No. 187, American Chemical Society, Washington, DC, 1986.
4. D. Dietrich, W. Keberle, and H. Witt, *Angew. Chem. Int. Ed.*, **9**, 40 (1970).
5. K. S. Hwang, C. Yang, and S. L. Cooper, *Polym. Eng. Sci.*, **21**, 1027 (1981).
6. M. Rutkowska and A. Eisenberg, *Macromolecules* **17**, 821 (1984).
7. M. Rutkowska and A. Eisenberg, *J. Appl. Polym. Sci.*, **29**, 755 (1984).
8. M. Rutkowska, *J. Appl. Polym. Sci.*, **31**, 1469 (1986).
9. P. W. Atkins, *Physical Chemistry*, Oxford University Press, Oxford, 1978, p. 472.
10. S. Bagrodia, M. R. Tant, G. L. Wilkes, and J. P. Kennedy, *Polymer*, **28**, 2207 (1987).
11. D. Tyagi, Ph.D. dissertation, Virginia Polytechnic Institute and State University, Dept. of Chemical Engineering, March 1985.
12. A. H. Willbourn, *Trans. Faraday Soc.*, **54**, 717 (1958).

Received May 10, 1988
Accepted July 29, 1988